Supporting Information:

Electronic Tunability and Mobility Anisotropy of Quasi-2D Perovskite Single Crystals with Varied Spacer Cations

*Yu Zhang[a], Mingzi Sun[b], Ning Zhou[a], Bolong Huang[*b], Huanping Zhou[*a]*

a. Y. Zhang, N. Zhou, Prof. H. P. Zhou

Beijing Key Laboratory for Theory and Technology of Advanced Battery Materials, Key Laboratory of Polymer Chemistry and Physics of Ministry of Education, BIC-ESAT, Department of Materials Science and Engineering, College of Engineering, Peking University, Beijing 100871, P. R. China.

b. Prof. B. L. Huang, M. Z. Sun

Department of Applied Biology and Chemical Technology, The Hong Kong Polytechnic University, Hung Hom, Kowloon, Hong Kong SAR, China

*Corresponding author: happy_zhou@pku.edu.cn, bhuang@polyu.edu.hk

Materials Preparation

All reagents were used as received without further purification. PbI_2 (99.985%, Alfa Aesar), HI aqueous solution (57% w/w, stabilized with 1.5% H_3PO_2, Alfa Aesar), γ-butyrolactone (99%, Aladdin). MAI, BAI, ALAI and PEAI were synthesized using the methods reported everywhere.

Synthesis of $XA_2MA_2Pb_3I_{10}$ (X=BA, ALA or PEA)single crystals

Precursors containing PbI_2, MAI, and XAI with specific ratios were dissolved in hydriodic acid (HI) solution (57% w/w in water) with specific volume at 100 °C. The solution was then slowly cooled to room temperature at a rate of 1 °C/h. The ratios are 1/0.75/0.5 mmol, 1/1.4/1.06 mmol, and 0.9/2.2/0.13 mmol in 1.4 ml, 0.9 ml and 2.4 ml of HI solution for $BA_2MA_2Pb_3I_{10}$, $ALA_2MA_2Pb_3I_{10}$ and $PEA_2MA_2Pb_3I_{10}$, respectively. The newly prepared single crystals were vacuum dried at 60 °C for 24 hours to remove the surface impurities such as HI. Further, we removed the surface layer of the single crystal by mechanical peeling to expose a new clean surface for characterization. The mechanical peeling method was achieved by sticking the two sides of the single crystal with tape and uncovering it evenly. Repeating this operation could also reduce the single crystal thickness.

Photodetector device fabrication

All the quasi-2D perovskite single crystal-based photodetectors were fabricated by simply thermally evaporating 100 nm thick Au electrodes on the smooth crystal surface with specific metal masks, defining a channel length (L) of 1000 μm and width (W) of 100 μm.

Characterization

SEM images were captured with S4800. X-ray Diffraction (XRD) data of single crystals were obtained on the PANalytical X'Pert Pro X-ray powder diffractometer with Cu Kα radiation (λ = 1.54050 Å). Absorption of perovskite single crystal particles were

measured by UV-Visible/NIR Spectrophotometer UH4150. Photoluminescence (PL) spectrum of single crystal particles were characterized by FLS980 (Edinburgh Instruments Ltd), and Time-Resolved Photoluminescence (TRPL) spectrum was obtained by 470 nm excitation wavelength. The dark current-voltage curve of Au/perovskite/Au device was measured through Keithley 4200 system to calculate the mobility of single crystals according to the Space-Charge-Limited Current (SCLC) model. The I−V measurements of single crystal photodetector devices were performed utilizing a Keithley 2636b parametric analyzer and a micromanipulator probe station (MPS 100S). Illumination was provided by a warm white LED lamp with adjustable power. Optical power meter was used to calibrate the light intensity.

Calculation setup

The operation of the calculation has been conducted through DFT within CASTEP packages[1]. We have chosen the PBE based with GGA functionals to describe the electronic exchange-correlation interaction[2-3]. For all the geometry relaxation of the perovskite models, the Broyden-Fletcher-Goldfarb-Shannon (BFGS) algorithm will be applied to optimize the residual Hellmann-Feynman forces to the range of 0.001 eV/A[4]. The total energy and the inter-ionic displacement will also be converged to 5×10^{-5} eV per atom and 0.005 Å per atom, respectively. The basis set will choose plane-wave cut-off energy with ultra fine quality and ultrasoft pseudopotential[5]. The spacing set of 0.07 $Å^{-1}$ is used in the Monkhost-Pack reciprocal space integration, which can achieve the self-consistent energy minimization within the maximum cycle settings[6]. For the $(BA)_2(MA)_2Pb_3I_{10}$ (n=3) model, we have applied the crystal structure parameters with atomic coordinates from previous study[7]. Since ALA molecule is similar chain with BA, we have replaced all the BA positions by ALA molecule for $(ALA)_2(MA)_2Pb_3I_{10}$ model construction. Due to much larger size of PEA molecule than normal short-chain organic spacer, the arrangement has been considered carefully[8-9]. The PEA molecules have been aligned in a displaced parallel stacking to avoid the strong repulsion induced by an energy unfavourable face-to-face overlap stacking with less stability[10-11].

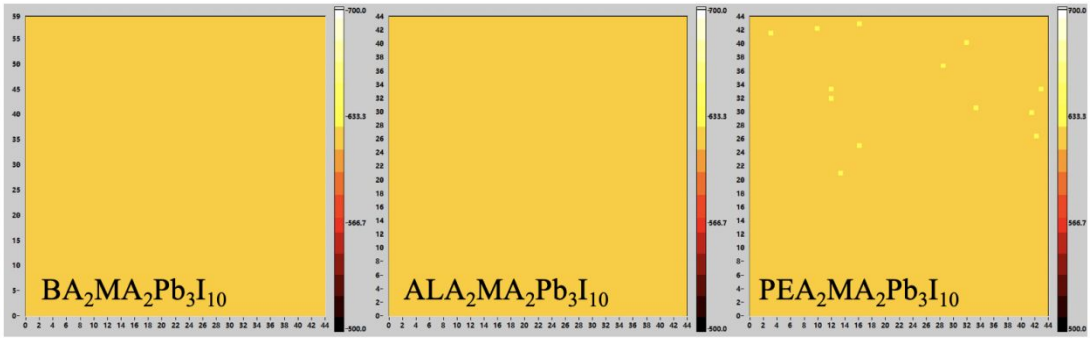

Figure S1 Typical PL mapping images of quasi-2D perovskite single crystals. (The unit of X-axis is “μm” and the unit of Y-axis is “nm”)

Due to the energy transfer between quasi-2D perovskites with different n values, steady-state PL cannot distinguish the phase purity. However, energy transfer will cause differences in the spatial distribution of photoluminescence, so PL mapping is a feasible way to judge phase purity. The results showed that the PL was very uniform, and there was no non-photoluminescence or abnormal photoluminescence area caused by energy transfer, which fully proved the purity of the obtained single crystals. The typical PL mapping images of each sample are shown in Figure S1. Among them, a few bright spots of $PEA_2MA_2Pb_3I_{10}$ were caused by its reduced band gap, which had been fully discussed in the manuscript.

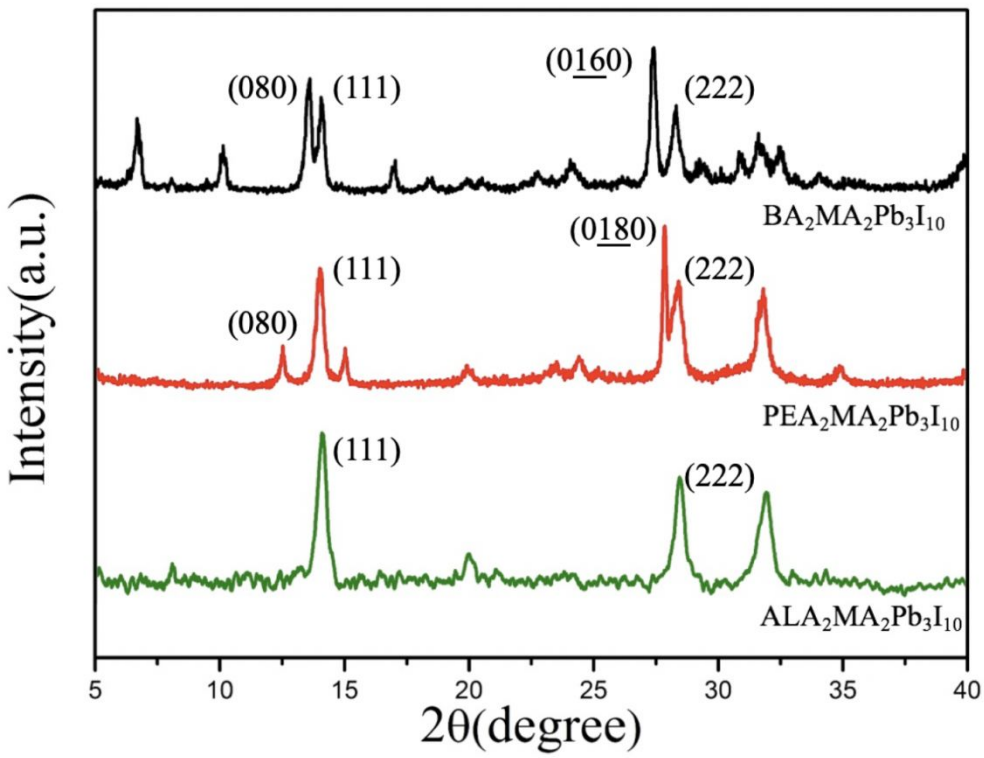

Figure S2 Powder X-ray diffraction (PXRD) of quasi-2D perovskite.

PXRD spectra changed significantly compared to single crystal XRD (Figure 1c). Firstly, the multi-order diffraction peaks of the layered structure were greatly weakened, and the (111) diffraction peaks appeared. Secondly, the diffraction intensity was greatly reduced, and the diffraction peaks were obviously broadened. From this, we can conclude that grinding destroyed the layered structure and preferred orientation of the quasi-2D perovskite single crystal, so its XRD pattern changed significantly. Therefore, the parameters we obtained from single crystal XRD, such as the layer spacing, were much more accurate than PXRD.

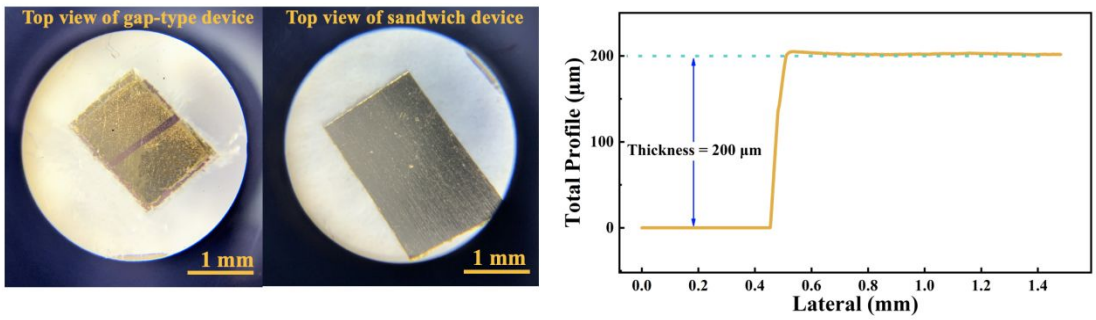

Figure S3 Optical images and thickness data of the devices.

The gap-type device was fabricated by simply thermally evaporating 100 nm thick Au electrodes on the smooth crystal surface with specific metal masks, defining a channel length (L) of 1000 μm and width (W) of 100 μm. To facilitate the preparation, one side of the single crystal was glued on the glass substrate with double-sided adhesive tape. (The residue on the edge of the device comes from the tape under the crystal.) For sandwich devices, we measured its thickness of 200 μm with a step profiler. The thickness of the device can be controlled by the mechanical peeling method.

References:

(1) Clark, S. J.; Segall, M. D.; Pickard, C. J.; Hasnip, P.; Probert, M. I. J.; Refson, K.; Payne, M. C. First Principles Methods Using CASTEP. *Zeitschrift Fur Kristallographie* 2005, *220*, 567-570.

(2) Perdew, J. P.; Chevary, J. A.; Vosko, S. H.; Jackson, K. A.; Pederson, M. R.; Singh, D. J.; Fiolhais, C. Atoms, Molecules, Solids, and Surfaces: Applications of the Generalized Gradient Approximation for Exchange and Correlation. *Phys. Rev. B* 1992, *46* (11), 6671-6687.

(3) Perdew, J. P.; Ernzerhof, M.; Burke, K. Rationale for Mixing Exact Exchange with Density Functional Approximations. *J. Chem. Phys.* 1996, *105* (22), 9982-9985.

(4) Head, J. D.; Zerner, M. C. A Broyden-Fletcher-Goldfarb-Shanno Optimization Procedure for Molecular Geometries. *Chem. Phys. Lett.* 1985, *122* (3), 264-270.

(5) Hasnip, P. J.; Pickard, C. J. Electronic Energy Minimisation with Ultrasoft Pseudopotentials. *Comput Phys Commun* 2006, *174* (1), 24-29.

(6) Probert, M. I. J.; Payne, M. C. Improving the Convergence of Defect Calculations in Supercells - an Ab Initio Study of the Neutral Silicon Vacancy. *Phys. Rev. B* 2003, *67* (7), 075204.

(7) Stoumpos, C. C.; Cao, D. H.; Clark, D. J.; Young, J.; Rondinelli, J. M.; Jang, J. I.; Hupp, J. T.; Kanatzidis, M. G. Ruddlesden–Popper Hybrid Lead Iodide Perovskite 2D Homologous Semiconductors. *Chem. Mater.* 2016, *28* (8), 2852-2867.

(8) Yang, S.; Niu, W.; Wang, A.; Fan, Z.; Chen, B.; Tan, C.; Lu, Q.; Zhang, H. Ultrathin Two-Dimensional Organic-Inorganic Hybrid Perovskite Nanosheets with Bright, Tunable Photoluminescence and High Stability. *Angew. Chem., Int. Ed.* 2017, *56* (15), 4252-4255.

(9) Azadmanjiri, J.; Wang, J.; Berndt, C. C.; Yu, A. 2D Layered Organic–Inorganic Heterostructures for Clean Energy Applications. *J. Mater. Chem. A* 2018, *6* (9), 3824-3849.

(10) Martinez, C. R.; Iverson, B. L. Rethinking the Term “Pi-Stacking”. *Chem. Sci.* 2012, *3* (7), 2191-2201.

(11) Hunter, C. A.; Sanders, J. K. M. The Nature of .pi.-.pi. Interactions. *J. Am. Chem. Soc.* 1990, *112* (14), 5525-5534.